

# Predictions of $\Upsilon(4S) \rightarrow h_b(1P, 2P)\pi^+\pi^-$ transitions

Yun-Hua Chen\*

*School of Mathematics and Physics, University of Science and Technology Beijing, Beijing 100083, China*

In this work, we study the contributions of the intermediate bottomoniumlike  $Z_b$  states and the bottom meson loops in the heavy quark spin flip transitions  $\Upsilon(4S) \rightarrow h_b(1P, 2P)\pi^+\pi^-$ . Depending on the constructive or destructive interferences between the  $Z_b$ -exchange and the bottom meson loops mechanisms, we predict two possible branching ratios for each process:  $\text{BR}_{\Upsilon(4S) \rightarrow h_b(1P)\pi^+\pi^-} \simeq (1.3_{-0.4}^{+0.9} \times 10^{-6})$  or  $(0.5_{-0.2}^{+0.5} \times 10^{-6})$ , and  $\text{BR}_{\Upsilon(4S) \rightarrow h_b(2P)\pi^+\pi^-} \simeq (9.2_{-1.2}^{+1.8} \times 10^{-10})$  or  $(4.4_{-0.3}^{+0.2} \times 10^{-10})$ . The bottom meson loops are found to play the leading role in the  $\Upsilon(4S) \rightarrow h_b(nP)\pi\pi$  transitions, while they can not produce decay rates comparable to the heavy quark spin conserved  $\Upsilon(4S) \rightarrow \Upsilon(1S, 2S)\pi\pi$  processes.

arXiv:1907.05547v1 [hep-ph] 12 Jul 2019

---

\*Electronic address: [yhchen@ustb.edu.cn](mailto:yhchen@ustb.edu.cn)

## I. INTRODUCTION

The hadronic transitions  $\Upsilon(mS) \rightarrow \Upsilon(lS)\pi\pi$  and  $\Upsilon(mS) \rightarrow h_b(nP)\pi\pi$  are important processes for understanding the heavy-quarkonium dynamics and low-energy QCD. The total spin of  $b\bar{b}$  system in  $\Upsilon(mS)$  and  $h_b(nP)$  are 1 and 0, respectively, thus in general the heavy quark spin flip  $\Upsilon(mS) \rightarrow h_b(nP)\pi\pi$  processes are expected to be suppressed compared with the heavy quark spin conserved  $\Upsilon(mS) \rightarrow \Upsilon(lS)\pi\pi$  processes. While in the decay processes  $\Upsilon(5S) \rightarrow \Upsilon(lS)\pi^+\pi^-$  ( $l = 1, 2, 3$ ) and  $\Upsilon(5S) \rightarrow h_b(nP)\pi^+\pi^-$  ( $n = 1, 2$ ) where the two charged bottomoniumlike resonances  $Z_b(10610)^\pm$  and  $Z_b(10650)^\pm$  were observed, the  $\Upsilon(5S) \rightarrow h_b(nP)\pi^+\pi^-$  proceed at a rate comparable to the  $\Upsilon(5S) \rightarrow \Upsilon(lS)\pi^+\pi^-$  processes [1, 2]. The mechanism that mitigates the expected suppression has remained controversial. In Refs. [3, 4], the production of the  $h_b(nP)$  at the  $\Upsilon(5S)$  is interpreted via bottom meson loops mechanism, while genuine  $S$ -matrix  $Z_b$  poles are required as in Ref. [5–8].

In this work, we will study that whether the bottom meson loops mechanism can produce the  $\Upsilon(4S) \rightarrow h_b(nP)\pi^+\pi^-$  transitions at the decay ratios comparable with  $\Upsilon(4S) \rightarrow \Upsilon(lS)\pi^+\pi^-$ . Since in the dipion emission processes of the  $\Upsilon(4S)$  the crossed-channel exchanged  $Z_b$  can not be on-shell, one may expect that these transitions are good channels to study the bottom meson loops' effect. In our previous works [9, 10], using the nonrelativistic effective field theory (NREFT) we calculated the effects of the bottom meson loops as well as the  $Z_b$ -exchange in the  $\Upsilon(4S) \rightarrow \Upsilon(1S, 2S)\pi\pi$  processes, and found that the experimental data can be described well. Here within the same theoretical scheme, we will calculate the contributions of the bottom meson loops and the  $Z_b$ -exchange in the  $\Upsilon(4S) \rightarrow h_b(nP)\pi^+\pi^-$  processes, and give the theoretical predictions of the decay branching ratios. We find that the effect of the bottom meson loops is dominant in the  $\Upsilon(4S) \rightarrow h_b(nP)\pi^+\pi^-$  process, while it can not produce a rate comparable with  $\Upsilon(4S) \rightarrow \Upsilon(1S, 2S)\pi^+\pi^-$ .

This paper is organized as follows. In Sec. II, the theoretical framework is described in detail. In Sec. III, we give the theoretical predictions for the decay branching fractions of  $\Upsilon(4S) \rightarrow h_b(1P, 2P)\pi^+\pi^-$ , and discuss the contributions of different mechanisms. A summary will be given in Sec. IV.

## II. THEORETICAL FRAMEWORK

### A. Lagrangians

To calculate the contribution of the mechanism  $\Upsilon(mS) \rightarrow Z_b\pi \rightarrow h_b(nP)\pi\pi$ , we need the effective Lagrangians for the  $Z_b\Upsilon\pi$  interaction and  $Z_bh_b\pi$  interaction [11],

$$\mathcal{L}_{Z_b\Upsilon\pi} = \sum_{j=1,2} C_{Z_{bj}\Upsilon(mS)\pi} \Upsilon^i(mS) \langle Z_{bj}^{i\dagger} u_\mu \rangle v^\mu + \text{h.c.}, \quad (1)$$

$$\mathcal{L}_{Z_bh_b\pi} = \sum_{j=1,2} g_{Z_{bj}h_b(nP)\pi} \epsilon_{ijk} \langle Z_{bj}^{i\dagger} u^j \rangle h_b^k + \text{h.c.}, \quad (2)$$

where  $Z_{b1}$  and  $Z_{b2}$  denote  $Z_b(10610)$  and  $Z_b(10650)$ , respectively, and  $v^\mu = (1, \mathbf{0})$  is the velocity of the heavy quark. The  $Z_b$  states are collected in the matrix as

$$Z_{bj}^i = \begin{pmatrix} \frac{1}{\sqrt{2}} Z_{bj}^{0i} & Z_{bj}^{+i} \\ Z_{bj}^{-i} & -\frac{1}{\sqrt{2}} Z_{bj}^{0i} \end{pmatrix}. \quad (3)$$

The pions as Goldstone bosons of the spontaneous breaking of the chiral symmetry can be parametrized as

$$u_\mu = i \left( u^\dagger \partial_\mu u - u \partial_\mu u^\dagger \right), \quad u = \exp \left( \frac{i\Phi}{\sqrt{2}F_\pi} \right),$$

$$\Phi = \begin{pmatrix} \frac{1}{\sqrt{2}}\pi^0 & \pi^+ \\ \pi^- & -\frac{1}{\sqrt{2}}\pi^0 \end{pmatrix}, \quad (4)$$

where  $F_\pi = 92.2 \text{ MeV}$  is the pion decay constant.

To calculate the box diagrams, we need the Lagrangian for the coupling of the  $\Upsilon$  to the bottom mesons and the coupling of the  $h_b$  to the bottom mesons [11, 12],

$$\mathcal{L}_{\Upsilon HH} = \frac{i g_{JHH}}{2} \langle J^\dagger H_a \sigma \cdot \overleftrightarrow{\partial} \bar{H}_a \rangle + \text{h.c.}, \quad (5)$$

$$\mathcal{L}_{h_b HH} = \frac{i g_1}{2} \langle h_b^\dagger H_a \sigma^i \bar{H}_a \rangle + \text{h.c.}, \quad (6)$$

where  $J \equiv \Upsilon \cdot \sigma + \eta_b$  denotes the heavy quarkonia spin multiplet,  $H_a = \mathbf{V}_a \cdot \sigma + P_a$  with  $P_a(V_a) = (B^{(*)-}, \bar{B}^{(*)0})$  collects the bottom mesons, and  $A \overleftrightarrow{\partial} B \equiv A(\overrightarrow{\partial} B) - (\overrightarrow{\partial} A)B$ . We also need the Lagrangian for the axial coupling of the pion fields to the bottom and antibottom mesons, which at the lowest order in heavy-flavor chiral perturbation theory is given by [13–17]

$$\mathcal{L}_{HH\Phi} = \frac{g_\pi}{2} \langle \bar{H}_a^\dagger \sigma \cdot \mathbf{u}_{ab} \bar{H}_b \rangle - \frac{g_\pi}{2} \langle H_a^\dagger H_b \sigma \cdot \mathbf{u}_{ba} \rangle, \quad (7)$$

where  $u^i = -\sqrt{2}\partial^i\Phi/F + \mathcal{O}(\Phi^3)$  denotes the three-vector components of  $u_\mu$  as defined in Eq. (4). Here we will use  $g_\pi = 0.492 \pm 0.029$  from a recent lattice QCD calculation [18].

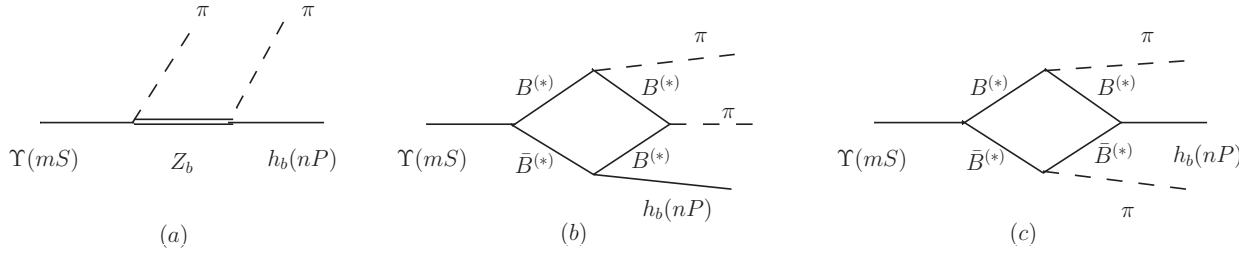


FIG. 1: Feynman diagrams considered for the  $\Upsilon(mS) \rightarrow h_b(nP)\pi\pi$  processes. The crossed diagrams of (a) and (b) are not shown explicitly.

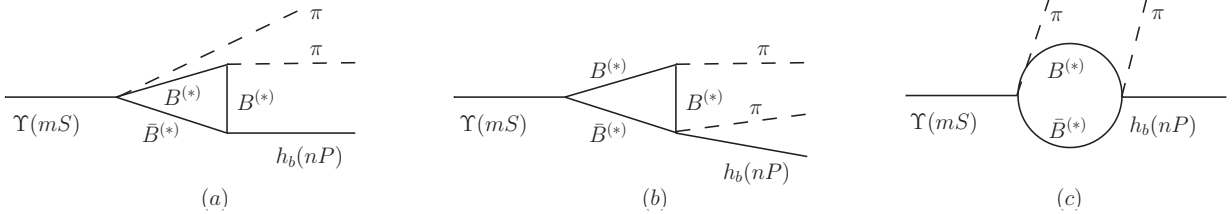


FIG. 2: The loop diagrams not considered in the calculations. The corresponding power counting arguments are given in the main text.

## B. Power counting of the loops

Since the  $\Upsilon(4S)$  meson is above the  $B\bar{B}$  threshold and decays predominantly into  $B\bar{B}$  pairs, the loop mechanism with intermediate bottom mesons may be important in the transitions  $\Upsilon(4S) \rightarrow h_b(nP)\pi^+\pi^-$ . Following the formalism set-up based on NREFT [12, 19, 20], we will analyze the power counting of different kinds of loops. In NREFT, the expansion parameter is the velocity of the intermediate heavy meson, namely  $\nu_X = \sqrt{|m_X - m_{B^{(*)}} - m_{\bar{B}^{(*)}}|/m_{B^{(*)}}}$ , which is small since the bottomonia  $X$  are close to the  $B^{(*)}\bar{B}^{(*)}$  thresholds. In this power counting, each nonrelativistic propagator scale as  $1/\nu^2$ , and the measure of one-loop integration scales as  $\int d^4l \sim \nu^5$ .

There are five different kinds of loop contributions, namely the box diagrams displayed in Fig. 1 (b), (c), the triangle diagrams displayed in Fig. 2 (a), (b), and the bubble loop in Fig. 2 (c). We analyze them one by one as follows:

First we analyze the power counting of the box diagrams, namely Fig. 1 (b), (c). As indicated in Eq. (7), the vertex of  $B^{(*)}B^{(*)}\pi$  is proportional to the external momentum of the pion  $q_\pi$ . The  $\Upsilon B^{(*)}\bar{B}^{(*)}$  vertex is in a  $P$ -wave, and the  $h_b B^{(*)}\bar{B}^{(*)}$  vertex is in an  $S$ -wave, so the loop momentum must contract with the external pion momentum and hence the  $P$ -wave vertex scales as  $\mathcal{O}(q_\pi)$ . Thus the box diagrams scales as  $\nu^5 q_\pi^3 / \nu^8 = q_\pi^3 / \nu^3$ .

As for the triangle diagram Fig. 2(a), the leading  $\Upsilon B^{(*)}\bar{B}^{(*)}\pi$  vertex given by  $g_{JHH\pi}\langle J\bar{H}_a^\dagger H_b^\dagger\rangle u_{ab}^0$  [21] is proportional to the energy of the pion,  $E_\pi \sim q_\pi$ . Therefore, Fig. 2(a) is counted as  $m_B\nu^5 q_\pi^2/\nu^6 = m_B q_\pi^2/\nu$ , where the factor  $m_B$  has been introduced to match the dimension with the scaling for the box diagrams.

In Fig. 2(b), the leading  $h_b B^{(*)}\bar{B}^{(*)}\pi$  vertex given by  $g_{h_b HH\pi}\langle h_b^\dagger H_a \sigma^j \bar{H}_b\rangle \epsilon_{ijk} u_{ab}^k$  [13] is proportional to the momentum the pion  $q_\pi$ . The loop momentum due to the  $\Upsilon B^{(*)}\bar{B}^{(*)}$  coupling has to contract with the external pion momentum. Thus, Fig. 2(b) scales as  $\nu^5 q_\pi^3/\nu^6 = q_\pi^3/\nu$ .

In Fig. 2(c), both the initial vertex and the final vertex are proportional to  $q_\pi$ , so the bubble loop scales as  $m_B\nu^5 q_\pi^2/\nu^4 = m_B q_\pi^2\nu$ .

Therefore, we expect that the ratios of the contributions of the box diagrams, triangle diagram Fig. 2(a) and 2(b), and the bubble loop Fig. 2(c) are

$$\begin{aligned} & \frac{q_\pi^3}{\nu^3} : \frac{m_B q_\pi^2}{\nu} : \frac{q_\pi^3}{\nu} : m_B q_\pi^2 \nu \\ = & 1 : \frac{m_B \nu^2}{q_\pi} : \nu^2 : \frac{m_B \nu^4}{q_\pi}, \end{aligned} \quad (8)$$

where  $q_\pi \simeq (m_{\Upsilon(4S)} - m_{h_b(nP)})/2$  and  $\nu = (\nu_{\Upsilon(4S)} + \nu_{h_b(nP)})/2$ , with  $\nu_{\Upsilon(4S)} \simeq 0.06$ ,  $\nu_{h_b(1P)} \simeq 0.35$ , and  $\nu_{h_b(2P)} \simeq 0.24$ . Thus for the  $\Upsilon(4S) \rightarrow h_b(1P)\pi^+\pi^-$  transition, the ratios in Eq. (8) are  $1 : 0.67 : 0.04 : 0.03$ . For the  $\Upsilon(4S) \rightarrow h_b(2P)\pi^+\pi^-$  transition, the ratios are  $1 : 0.75 : 0.02 : 0.02$ . Therefore according to the power counting the box diagrams and the triangle diagram in Fig. 2(a) are dominant among the loop contributions, and they are of the same order. While the  $\Upsilon(4S)$  is below the  $B^{(*)}\bar{B}^{(*)}\pi$  threshold and the coupling  $g_{JHH\pi}$  in the triangle diagram Fig. 2(a) is unknown. Thus for a rough estimation of the loop contributions, we will only calculate the box diagrams in the present study. Note that all the box and triangle loop contributions discussed here are ultraviolet-finite, and do not require the additional introduction of counterterms.

### C. Tree-level amplitudes and box diagram calculation

The decay amplitude for

$$\Upsilon(mS)(p_a) \rightarrow h_b(nP)(p_b)\pi(p_c)\pi(p_d) \quad (9)$$

is described in terms of the Mandelstam variables

$$s = (p_c + p_d)^2, \quad t = (p_a - p_c)^2, \quad u = (p_a - p_d)^2. \quad (10)$$

Using the effective Lagrangians in Eqs. (1) and (2), the tree amplitude of  $\Upsilon(mS) \rightarrow Z_b\pi \rightarrow h_b(nP)\pi\pi$  can be obtained

$$M_{Zb} = \frac{2\sqrt{m_{\Upsilon(mS)}m_{h_b(nP)}}}{F_\pi^2} \epsilon_{abj} \epsilon_{\Upsilon(mS)}^a \epsilon_{h_b(nP)}^b \sum_{i=1,2} m_{Z_{bi}} C_{Z_{bi}} \Upsilon(mS) \pi g_{Z_{bi}h_b(nP)\pi} \left\{ p_c^0 p_d^j \frac{1}{t - m_{Z_{bi}}^2} + p_d^0 p_c^j \frac{1}{u - m_{Z_{bi}}^2} \right\}. \quad (11)$$

Notice that the nonrelativistic normalization factor  $\sqrt{m_Y}$  has been multiplied to the amplitude for every heavy particle, with  $Y = \Upsilon(mS), h_b(nP), Z_{bi}$ . The widths of the  $Z_b$  states are neglected in the present study, since they are of the order of 10 MeV and are much smaller than the difference between the  $Z_b$  masses and the  $\Upsilon(mS)\pi/h_b(nP)\pi$  threshold.

Now we discuss the calculation of the box diagrams. In the box diagrams Fig. 1(b) and (c), we denote the top left intermediate bottom meson as  $M1$ , and the other intermediate bottom mesons as  $M2, M3$ , and  $M4$ , in counterclockwise order. Concerned with the pseudoscalar or vector content of  $[M1, M2, M3, M4]$ , there are twelve possible patterns and we number them in order: 1,  $[PPPV]$ ; 2,  $[PPVV]$ ; 3,  $[PVPV]$ ; 4,  $[PVVP]$ ; 5,  $[VVPP]$ ; 6,  $[VPVP]$ ; 7,  $[VPPV]$ ; 8,  $[PVVV]$ ; 9,  $[VPVV]$ ; 10,  $[VVPV]$ ; 11,  $[VVVP]$ ; 12,  $[VVVV]$ . For each pattern, we also need to consider six possibilities of different flavor of the intermediate bottom mesons:  $[B^{(*)+}, B^{(*)-}, B^{(*)+}, B^{(*)0}]$ ,  $[B^{(*)+}, B^{(*)-}, \bar{B}^{(*)0}, B^{(*)0}]$ ,  $[B^{(*)0}, \bar{B}^{(*)0}, B^{(*)0}, B^{(*)+}]$ ,  $[B^{(*)-}, B^{(*)+}, B^{(*)-}, \bar{B}^{(*)0}]$ ,  $[\bar{B}^{(*)0}, B^{(*)0}, B^{(*)+}, B^{(*)-}]$ , and  $[\bar{B}^{(*)0}, B^{(*)0}, \bar{B}^{(*)0}, B^{(*)-}]$ . The full amplitude contains the sum of all possible ones.

For the tensor reduction of the loop integrals it is convenient to define  $\mathbf{q} = -\mathbf{p}_b$  and the perpendicular momentum  $\mathbf{q}_\perp = \mathbf{p}_c - \mathbf{q}(\mathbf{q} \cdot \mathbf{p}_c)/\mathbf{q}^2$ , which satisfy  $\mathbf{q} \cdot \mathbf{q}_\perp = 0$ . The result of the amplitude of the box diagrams can be written as

$$M_{\text{loop}} = \epsilon_{\Upsilon(mS)}^a \epsilon_{h_b(nP)}^b \left\{ \epsilon_{abi} q^i A_1 + \epsilon_{abi} q_\perp^i A_2 + \epsilon_{bij} q^i q_\perp^j q_\perp^a A_3 + \epsilon_{bij} q^i q_\perp^j q_\perp^a A_4 + \epsilon_{aij} q^i q_\perp^j q_\perp^b A_5 + \epsilon_{aij} q^i q_\perp^j q_\perp^b A_6 \right\}. \quad (12)$$

Details on the analytic calculation of the box diagrams and the explicit expressions of  $A_i$  ( $i = 1, 2, \dots, 6$ ) are given in Appendix A.

The decay width for  $\Upsilon(mS) \rightarrow h_b(nP)\pi\pi$  is given by

$$\Gamma = \int_{s_-}^{s_+} \int_{t_-}^{t_+} \frac{|M_{Zb} + M_{\text{loop}}|^2 ds dt}{768\pi^3 m_{\Upsilon(mS)}^3}, \quad (13)$$

where the lower and upper limits are given as

$$\begin{aligned}
s_- &= 4m_\pi^2, \\
s_+ &= (m_{\Upsilon(mS)} - m_{h_b(nP)})^2, \\
t_\pm &= \frac{1}{4s} \left\{ (m_{\Upsilon(mS)}^2 - m_{h_b(nP)}^2)^2 - \left[ \lambda^{\frac{1}{2}}(s, m_\pi^2, m_\pi^2) \mp \lambda^{\frac{1}{2}}(m_{\Upsilon(mS)}^2, s, m_{h_b(nP)}^2) \right]^2 \right\}, \\
\lambda(a, b, c) &= a^2 + b^2 + c^2 - 2(ab + ac + bc).
\end{aligned} \tag{14}$$

### III. PHENOMENOLOGICAL DISCUSSION

To estimate the contribution of the  $Z_b$ -exchange mechanism we need to know the coupling strengths of  $Z_b\Upsilon(4S)\pi$  and  $Z_b h_b(nP)\pi$ . The mass difference between  $Z_b(10610)$  and  $Z_b(10650)$  is much smaller than the difference between their masses and the  $\Upsilon(mS)\pi/h_b(nP)\pi$  threshold, and they have the same quantum numbers and thus the same coupling structures as dictated by Eqs. (1) and (2). Therefore it is very difficult to distinguish their effects from each other in the dipion transitions of  $\Upsilon(4S)$ , so we only use one  $Z_b$ , the  $Z_b(10610)$ , which approximately combine both  $Z_b$  states' effects. In Ref. [10], we have studied the  $\Upsilon(4S) \rightarrow \Upsilon(mS)\pi\pi$  processes to extract the coupling constant  $|C_{Z_b\Upsilon(4S)\pi}| = (3.3 \pm 0.1) \times 10^{-3}$ , which containing effects from both  $Z_b$  states. For the couplings of  $Z_b h_b(nP)\pi$ , in principle they can be extracted from the partial widths of the  $Z_b$  states decay into  $h_b(nP)\pi$  ( $n = 1, 2$ )

$$|g_{Z_b h_b \pi}| = \left\{ \frac{6\pi F_\pi^2 m_{Z_b} \Gamma_{Z_b \rightarrow h_b \pi}}{|\mathbf{p}_f|^3 m_{h_b}} \right\}^{\frac{1}{2}}, \tag{15}$$

where  $|\mathbf{p}_f| \equiv \lambda^{1/2}(m_{Z_b}^2, m_{h_b}^2, m_\pi^2)/(2m_{Z_b})$ . The preliminary results for the branching fractions of the decays of both  $Z_b$  states into  $h_b(nP)\pi$  ( $n = 1, 2$ ) have been given in [22], where the  $Z_b$  line shapes were described using Breit-Wigner forms. If we naively use these branching fractions, we would obtain

$$\begin{aligned}
|g_{Z_{b1} h_b(1P)\pi}^{\text{naive}}| &= 0.017 \pm 0.003, \\
|g_{Z_{b2} h_b(1P)\pi}^{\text{naive}}| &= 0.017 \pm 0.003, \\
|g_{Z_{b1} h_b(2P)\pi}^{\text{naive}}| &= 0.065 \pm 0.016, \\
|g_{Z_{b2} h_b(2P)\pi}^{\text{naive}}| &= 0.067 \pm 0.014.
\end{aligned} \tag{16}$$

Here all the  $Z_b h_b \pi$  couplings are labeled by a superscript ‘naive’ since this is not the appropriate way to extract the coupling strengths in this case; the  $Z_b$  states are very close to the  $B^{(*)}\bar{B}^*$

thresholds, and thus the Flatté parametrization for the  $Z_b$  spectral functions should be used, which will lead to much larger partial widths into  $(b\bar{b}\pi)$  channels, and thus the relevant coupling strengths. As analyzed in Ref. [23], we expect that the  $|g_{Z_b h_b \pi}|^2$  should be about 1 order of magnitude larger than the naive one, so for a rough estimation we will use three times the results from Eq. (16), namely

$$\begin{aligned} |g_{Z_b h_b(1P)\pi}| &\simeq 0.051, \\ |g_{Z_b h_b(2P)\pi}| &\simeq 0.198. \end{aligned} \quad (17)$$

In the calculation of the box diagrams, the coupling strength  $g_{JHH(4S)}$  can be extracted from the measured open-bottom decay widths of the  $\Upsilon(4S)$ , and we have  $g_{JHH(4S)} = 1.43 \pm 0.01 \text{ GeV}^{-3/2}$ . For the  $h_b B^* \bar{B}^*$  coupling  $g_1$ , we can use the results from Ref. [11]. In [11], the  $Z_b$ -exchange mechanism in the  $\Upsilon(5S) \rightarrow h_b(1P, 2P)\pi\pi$  processes has been studied assuming the  $Z_b$  states are  $B^{(*)}\bar{B}^*$  bound states, and the physical coupling of the  $Z_b$  states to the bottom and anti-bottom mesons,  $z_1$ , as well as the product  $g_1 z_1$  have been determined.<sup>1</sup> Using their results  $z_1 = 0.75_{-0.11}^{+0.08} \text{ GeV}^{-1/2}$  and  $g_1 z_1 = 0.40 \pm 0.06 \text{ GeV}^{-1}$ , we can extract that  $g_1 = 0.53_{-0.13}^{+0.19} \text{ GeV}^{-1/2}$ .

Using the coupling strengths above, we can predict the decay branching fractions of  $\Upsilon(4S) \rightarrow h_b(1P, 2P)\pi^+\pi^-$ . Depending on the sign of the couplings in Eq. (17), the interferences can be constructive or destructive between the  $Z_b$ -exchange and box graph mechanisms, so there are two possible results for each process

$$\begin{aligned} \text{BR}_{\Upsilon(4S) \rightarrow h_b(1P)\pi^+\pi^-} &\simeq (1.3_{-0.4}^{+0.9} \times 10^{-6}) \quad \text{or} \quad (0.5_{-0.2}^{+0.5} \times 10^{-6}), \\ \text{BR}_{\Upsilon(4S) \rightarrow h_b(2P)\pi^+\pi^-} &\simeq (9.2_{-1.2}^{+1.8} \times 10^{-10}) \quad \text{or} \quad (4.4_{-0.3}^{+0.2} \times 10^{-10}). \end{aligned} \quad (18)$$

We find that the  $\text{BR}_{\Upsilon(4S) \rightarrow h_b(1P)\pi^+\pi^-}$  is at least one order of magnitude smaller than the branching fractions  $\text{BR}_{\Upsilon(4S) \rightarrow \Upsilon(1S, 2S)\pi^+\pi^-}$ , which are about  $8 \times 10^{-5}$  given in PDG [24], and the  $\text{BR}_{\Upsilon(4S) \rightarrow h_b(2P)\pi^+\pi^-}$  is tiny due to the very small phase space. To illustrate the effects of the  $Z_b$ -exchange and box graph mechanisms in  $\Upsilon(4S) \rightarrow h_b(1P)\pi\pi$ , we give the predictions only including the  $Z_b$ -exchange terms or only including the box diagrams

$$\begin{aligned} \text{BR}_{\Upsilon(4S) \rightarrow h_b(1P)\pi^+\pi^-}^{Z_b} &= 0.2_{-0.1}^{+0.1} \times 10^{-6}, \\ \text{BR}_{\Upsilon(4S) \rightarrow h_b(1P)\pi^+\pi^-}^{\text{Box}} &= 0.8_{-0.3}^{+0.7} \times 10^{-6}. \end{aligned} \quad (19)$$

<sup>1</sup> In [11], in order to reduce the number of free parameters, the couplings of  $h_b(1P)B^*\bar{B}^*$  and  $h_b(2P)B^*\bar{B}^*$  are assumed to be the same.



The  $\Upsilon(mS) \rightarrow h_b(nP)\pi\pi$  are heavy quark spin flip processes and they are forbidden in the heavy quark limit. We have checked that in the heavy quark limit, *i.e.*  $m_B = m_{B^*}$ , all the box diagrams are cancelled with each other so the bottomed loops contribute nothing to the  $\Upsilon(mS) \rightarrow h_b(nP)\pi\pi$  transitions. With the small mass splitting of  $B$  and  $B^*$  in the real world, in Eq. (19) one observes that though the bottomed meson loops contribute dominantly in the  $\Upsilon(4S) \rightarrow h_b(1P)\pi\pi$  transition, they do not produce a rate comparable to the heavy quark spin conserved  $\Upsilon(4S) \rightarrow \Upsilon(1S, 2S)\pi\pi$  transitions. Thus the experimental measurement of the  $\Upsilon(4S) \rightarrow h_b(1P)\pi\pi$  transition in the future can be useful to identification of the bottomed meson loops' role in this kind of heavy quark spin flip processes.

#### IV. CONCLUSIONS

In this paper, we study the effects of  $Z_b$  exchange and bottom meson loops in the heavy quark spin flip transitions  $\Upsilon(4S) \rightarrow h_b(nP)\pi\pi$  ( $n = 1, 2$ ). The bottom meson loops are treated in the NREFT scheme, in which the dominant box diagrams are taken into account. We find that the bottom meson loops play a major role in the  $\Upsilon(4S) \rightarrow h_b(1P, 2P)\pi\pi$  transitions, while they can not produce decay rates comparable to the heavy quark spin conserved  $\Upsilon(4S) \rightarrow \Upsilon(1S, 2S)\pi\pi$  processes. The theoretical prediction of the decay rate of  $\Upsilon(4S) \rightarrow h_b(1P)\pi\pi$  in this work may be useful for identification of the effect of the bottom meson loops with future experimental data.

#### Acknowledgments

We are grateful to Martin Cleven for the collaboration at the early stages of this study. We acknowledge Guo-Ying Chen, Meng-Lin Du, and Qian Wang for helpful discussions, and Feng-Kun Guo for a careful reading of the manuscript and valuable comments. This research is supported in part by the Fundamental Research Funds for the Central Universities under Grant No. 06500077.

#### Appendix A: Remarks on the box diagrams and four-point integrals

In this appendix, first we will discuss the parametrization and simplification of the scalar four-point integrals in the box diagrams. Then we introduce a tensor reduction scheme to deal with higher-rank loop integrals. Finally, we give the amplitude of the box diagrams for the  $\Upsilon(mS) \rightarrow h_b(nP)\pi\pi$  process.

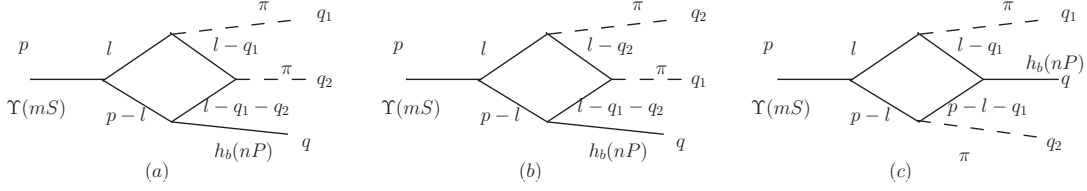


FIG. 3: Kinematics used in the calculation of the four-point integrals.

### 1. Scalar four-point integrals

For the first topology as shown in Fig. 3, the scalar integral evaluated for the initial bottomonium at rest ( $p = (M, \mathbf{0})$ ) reads

$$\begin{aligned}
J_1^{(0)} &\equiv i \int \frac{d^4 l}{(2\pi)^4} \frac{1}{[l^2 - m_1^2 + i\epsilon][(p-l)^2 - m_2^2 + i\epsilon][(l-q_1-q_2)^2 - m_3^2 + i\epsilon][(l-q_1)^2 - m_4^2 + i\epsilon]} \\
&\simeq \frac{-i}{16m_1 m_2 m_3 m_4} \int \frac{d^4 l}{(2\pi)^4} \frac{1}{\left[l^0 - \frac{l^2}{2m_1} - m_1 + i\epsilon\right] \left[l^0 - M + \frac{l^2}{2m_2} + m_2 - i\epsilon\right]} \\
&\times \frac{1}{\left[l^0 - q_1^0 - q_2^0 - \frac{(\mathbf{1}+\mathbf{q})^2}{2m_3} - m_3 + i\epsilon\right] \left[l^0 - q_1^0 - \frac{(\mathbf{1}-\mathbf{q}_1)^2}{2m_4} - m_4 + i\epsilon\right]}. \tag{A1}
\end{aligned}$$

Performing the contour integration, we find

$$-\frac{\mu_{12}\mu_{23}\mu_{24}}{2m_1 m_2 m_3 m_4} \int \frac{d^3 l}{(2\pi)^3} \frac{1}{[\mathbf{l}^2 + c_{12} - i\epsilon][\mathbf{l}^2 + 2\frac{\mu_{23}}{m_3} \mathbf{l} \cdot \mathbf{q} + c_{23} - i\epsilon][\mathbf{l}^2 - 2\frac{\mu_{24}}{m_4} \mathbf{l} \cdot \mathbf{q}_1 + c_{24} - i\epsilon]}, \tag{A2}$$

where we defined

$$\begin{aligned}
c_{12} &\equiv 2\mu_{12} (m_1 + m_2 - M), \quad c_{23} \equiv 2\mu_{23} \left( m_2 + m_3 - M + q_1^0 + q_2^0 + \frac{\mathbf{q}^2}{2m_3} \right), \\
c_{24} &\equiv 2\mu_{24} \left( m_2 + m_4 - M + q_1^0 + \frac{\mathbf{q}_1^2}{2m_4} \right), \quad \mu_{ij} = \frac{m_i m_j}{m_i + m_j}. \tag{A3}
\end{aligned}$$

The second topology in Fig. 3 is just the crossed diagram of the first topology with  $q_1 \leftrightarrow q_2$ , so the scalar integral reads

$$J_2^{(0)} = -\frac{\mu_{12}\mu_{23}\mu_{24}}{2m_1 m_2 m_3 m_4} \int \frac{d^3 l}{(2\pi)^3} \frac{1}{[\mathbf{l}^2 + c_{12} - i\epsilon][\mathbf{l}^2 + 2\frac{\mu_{23}}{m_3} \mathbf{l} \cdot \mathbf{q} + c_{23} - i\epsilon][\mathbf{l}^2 - 2\frac{\mu_{24}}{m_4} \mathbf{l} \cdot \mathbf{q}_2 + c'_{24} - i\epsilon]}, \tag{A4}$$

where

$$c'_{24} \equiv 2\mu_{24} \left( m_2 + m_4 - M + q_2^0 + \frac{\mathbf{q}_2^2}{2m_4} \right). \tag{A5}$$

For the third topology we have

$$\begin{aligned}
J_3^{(0)} &\equiv i \int \frac{d^4 l}{(2\pi)^4} \frac{1}{[l^2 - m_1^2 + i\epsilon][(p-l)^2 - m_2^2 + i\epsilon][(p-q_2-l)^2 - m_3^2 + i\epsilon][(l-q_1)^2 - m_4^2 + i\epsilon]} \\
&\simeq \frac{-i}{16m_1 m_2 m_3 m_4} \int \frac{d^4 l}{(2\pi)^4} \frac{1}{\left[l^0 - \frac{l^2}{2m_1} - m_1 + i\epsilon\right] \left[l^0 - M + \frac{l^2}{2m_2} + m_2 - i\epsilon\right]} \\
&\times \frac{1}{\left[l^0 + q_2^0 - M + \frac{(1+\mathbf{q}_2)^2}{2m_3} + m_3 - i\epsilon\right] \left[l^0 - q_1^0 - \frac{(1-\mathbf{q}_1)^2}{2m_4} - m_4 + i\epsilon\right]}. \tag{A6}
\end{aligned}$$

Performing the contour integration, we find

$$\begin{aligned}
&-\frac{\mu_{12}\mu_{34}}{2m_1 m_2 m_3 m_4} \int \frac{d^3 l}{(2\pi)^3} \frac{1}{[\mathbf{l}^2 + d_{12} - i\epsilon][\mathbf{l}^2 - 2\frac{\mu_{34}}{m_4} \mathbf{l} \cdot \mathbf{q}_1 - 2\frac{\mu_{34}}{m_3} \mathbf{l} \cdot \mathbf{q}_2 + d_{34} - i\epsilon]} \\
&\times \left[ \frac{\mu_{24}}{[\mathbf{l}^2 - 2\frac{\mu_{24}}{m_4} \mathbf{l} \cdot \mathbf{q}_1 + d_{24} - i\epsilon]} + \frac{\mu_{13}}{[\mathbf{l}^2 + 2\frac{\mu_{13}}{m_3} \mathbf{l} \cdot \mathbf{q}_2 + d_{13} - i\epsilon]} \right], \tag{A7}
\end{aligned}$$

where we defined

$$\begin{aligned}
d_{12} &\equiv 2\mu_{12}(m_1 + m_2 - M), & d_{34} &\equiv 2\mu_{34} \left( m_3 + m_4 - q^0 + \frac{\mathbf{q}_1^2}{2m_4} + \frac{\mathbf{q}_2^2}{2m_3} \right), \\
d_{24} &\equiv 2\mu_{24} \left( m_2 + m_4 - M + q_1^0 + \frac{\mathbf{q}_1^2}{2m_4} \right), & d_{13} &\equiv 2\mu_{13} \left( m_1 + m_3 - M + q_2^0 + \frac{\mathbf{q}_2^2}{2m_3} \right). \tag{A8}
\end{aligned}$$

In all the three cases the remaining three-dimensional momentum integration will be carried out numerically.

## 2. Tensor reduction

Since the  $\Upsilon B^{(*)} \bar{B}^{(*)}$  vertex scales with the momentum of the bottom meson pair, for topology I we have to deal with

$$\frac{-\mu_{12}\mu_{23}\mu_{24}}{2m_1 m_2 m_3 m_4} \int \frac{d^3 l}{(2\pi)^3} \frac{f(l)}{[\mathbf{l}^2 + c_{12} - i\epsilon][\mathbf{l}^2 + 2\frac{\mu_{23}}{m_3} \mathbf{l} \cdot \mathbf{q} + c_{23} - i\epsilon][\mathbf{l}^2 - 2\frac{\mu_{24}}{m_4} \mathbf{l} \cdot \mathbf{q}_1 + c_{24} - i\epsilon]}, \tag{A9}$$

where  $f(l) = \{1, l^i\}$  for the fundamental scalar and vector integrals, respectively. A convenient parametrization of the tensor reduction reads

$$\begin{aligned}
J_1^{(1)i} &= \frac{-\mu_{12}\mu_{23}\mu_{24}}{2m_1 m_2 m_3 m_4} \int \frac{d^3 l}{(2\pi)^3} \frac{l^i}{[\mathbf{l}^2 + c_1 - i\epsilon][\mathbf{l}^2 - 2\frac{\mu_{23}}{m_3} \mathbf{l} \cdot \mathbf{q} + c_2 - i\epsilon][\mathbf{l}^2 - 2\frac{\mu_{24}}{m_4} \mathbf{l} \cdot \mathbf{q}_1 + c_3 - i\epsilon]} \\
&\equiv q^i J_1^{(1)} + q_{1\perp}^i J_1^{(2)}, \tag{A10}
\end{aligned}$$

where  $\mathbf{q}_{1\perp} = \mathbf{q}_1 - \mathbf{q}(\mathbf{q} \cdot \mathbf{q}_1)/\mathbf{q}^2$ . The expressions of the scalar integrals  $J_1^{(r)}$  can easily be disentangled and have to be evaluated numerically. The corresponding expressions for topology II and III can be obtained by changing the denominators accordingly.

### 3. Amplitudes

We define the scalar integrals  $J1(i, r, k)$  based on the  $J_1^{(r)}$  in the tensor reduction of vector integral in Eq. (A10), where  $i = 1, 2, 3$  denotes the three topologies of box diagrams as shown in Fig. 3,  $r = 1, 2$  refers to the two components  $J_1^{(r)}$ , and  $k = 1, 2, \dots, 12$  represents the twelve patterns with different pseudoscalar or vector content of the intermediate bottom mesons in  $[M1, M2, M3, M4]$  as displayed in Sec. II C.

We give the amplitude of the box diagrams for the  $\Upsilon(mS) \rightarrow h_b(nP)\pi\pi$  process, namely the  $A_l (l = 1, 2, \dots, 6)$  in the Eq. (12).

$$\begin{aligned}
A_1 = & \frac{8g_1g_{JHH}g_\pi^2}{F_\pi^2\mathbf{q}^2} \left\{ \mathbf{q}^2 \left\{ \mathbf{p}_c \cdot \mathbf{p}_d [J1(1, 1, 3) + J1(2, 1, 3) + J1(3, 1, 8)] + \mathbf{p}_c \cdot \mathbf{q} [J1(1, 1, 9) + J1(1, 1, 11) \right. \right. \\
& - J1(2, 1, 12) + J1(3, 1, 9) + J1(3, 1, 11)] + \mathbf{q}_\perp^2 [J1(1, 2, 9) + J1(1, 2, 11) - J1(2, 2, 12) + J1(3, 2, 9) \\
& + J1(3, 2, 11)] \left. \right\} + \mathbf{p}_c \cdot \mathbf{q} \left\{ \mathbf{p}_c \cdot \mathbf{q} [J1(1, 1, 9) + J1(1, 1, 11) - J1(2, 1, 12) + J1(3, 1, 9) + J1(3, 1, 11)] \right. \\
& + \mathbf{p}_d \cdot \mathbf{q} [J1(1, 1, 12) - J1(2, 1, 9) - J1(2, 1, 11) + J1(3, 1, 10)] + \mathbf{q}_\perp^2 [J1(1, 2, 9) + J1(1, 2, 11) \\
& - J1(1, 2, 12) + J1(2, 2, 9) + J1(2, 2, 11) - J1(2, 2, 12) + J1(3, 2, 9) - J1(3, 2, 10) + J1(3, 2, 11)] \left. \right\} ,
\end{aligned}$$

$$\begin{aligned}
A_2 = & \frac{8g_1g_{JHH}g_\pi^2}{F_\pi^2} \left\{ \mathbf{p}_c \cdot \mathbf{p}_d [J1(1, 2, 3) + J1(2, 2, 3) + J1(3, 2, 8)] + \mathbf{p}_c \cdot \mathbf{q} [J1(1, 1, 9) + J1(1, 1, 11) \right. \\
& - J1(2, 1, 12) + J1(3, 1, 9) + J1(3, 1, 11)] + \mathbf{p}_d \cdot \mathbf{q} [J1(1, 1, 12) - J1(2, 1, 9) - J1(2, 1, 11) \\
& + J1(3, 1, 10)] + \mathbf{q}_\perp^2 [J1(1, 2, 9) + J1(1, 2, 11) - J1(1, 2, 12) + J1(2, 2, 9) + J1(2, 2, 11) \\
& - J1(2, 2, 12) + J1(3, 2, 9) - J1(3, 2, 10) + J1(3, 2, 11)] \left. \right\} , \tag{A12}
\end{aligned}$$

$$\begin{aligned}
A_3 = & -\frac{8g_1g_{JHH}g_\pi^2}{F_\pi^2\mathbf{q}^2} \left\{ \mathbf{q}^2 [ - J1(1, 1, 9) + J1(1, 1, 11) - J1(1, 1, 12) - J1(1, 2, 2) + J1(1, 2, 9) + J1(1, 2, 10) \right. \\
& + J1(1, 2, 12) - J1(2, 1, 9) + J1(2, 1, 11) - J1(2, 1, 12) + J1(2, 2, 2) - J1(2, 2, 10) - J1(2, 2, 11) \\
& - J1(3, 1, 9) - J1(3, 1, 10) + J1(3, 1, 11) - J1(3, 2, 2) + J1(3, 2, 9) + J1(3, 2, 10) + J1(3, 2, 12)] \\
& + \mathbf{p}_c \cdot \mathbf{q} [J1(1, 2, 9) - J1(1, 2, 11) + J1(1, 2, 12) + J1(2, 2, 9) - J1(2, 2, 11) + J1(2, 2, 12) \\
& + J1(3, 2, 9) + J1(3, 2, 10) - J1(3, 2, 11)] \left. \right\} , \tag{A13}
\end{aligned}$$

$$\begin{aligned}
A_4 = & \frac{8g_1g_{JHH}g_\pi^2}{F_\pi^2\mathbf{q}^4} \left\{ \mathbf{q}^4 [J1(1,1,2) - J1(1,1,10) - J1(1,1,11) - J1(2,1,2) + J1(2,1,9) + J1(2,1,10) \right. \\
& + J1(2,1,12) + J1(3,1,2) - J1(3,1,11) - J1(3,1,12)] + \mathbf{q}^2 \mathbf{p}_c \cdot \mathbf{q} [J1(1,1,9) - J1(1,1,11) \\
& + J1(1,1,12) - J1(1,2,9) + J1(1,2,11) - J1(1,2,12) + J1(2,1,9) - J1(2,1,11) + J1(2,1,12) \\
& - J1(2,2,9) + J1(2,2,11) - J1(2,2,12) + J1(3,1,9) + J1(3,1,10) - J1(3,1,11) - J1(3,2,9) \\
& - J1(3,2,10) + J1(3,2,11)] - (\mathbf{p}_c \cdot \mathbf{q})^2 [J1(1,2,9) - J1(1,2,11) + J1(1,2,12) + J1(2,2,9) \\
& \left. - J1(2,2,11) + J1(2,2,12) + J1(3,2,9) + J1(3,2,10) - J1(3,2,11)] \right\}, \tag{A14}
\end{aligned}$$

$$\begin{aligned}
A_5 = & \frac{8g_1g_{JHH}g_\pi^2}{F_\pi^2\mathbf{q}^2} \left\{ \mathbf{q}^2 [-J1(1,1,6) + J1(1,2,8) + J1(1,2,10) - J1(2,1,6) + J1(2,2,6) - J1(2,2,8) \right. \\
& - J1(2,2,10) - J1(3,1,3) + J1(3,1,6) - J1(3,1,8) + J1(3,2,3) + J1(3,2,12)] + \mathbf{p}_c \cdot \mathbf{q} \\
& \left. [J1(1,2,6) + J1(2,2,6) + J1(3,2,3) - J1(3,2,6) + J1(3,2,8)] \right\}, \tag{A15}
\end{aligned}$$

$$\begin{aligned}
A_6 = & -\frac{8g_1g_{JHH}g_\pi^2}{F_\pi^2\mathbf{q}^4} \left\{ \mathbf{q}^4 [J1(1,1,6) - J1(1,1,8) - J1(1,1,10) + J1(2,1,8) + J1(2,1,10) - J1(3,1,6) \right. \\
& + J1(3,1,8) - J1(3,1,12)] + \mathbf{q}^2 \mathbf{p}_c \cdot \mathbf{q} [J1(1,1,6) - J1(1,2,6) + J1(2,1,6) - J1(2,2,6) + J1(3,1,3) \\
& - J1(3,1,6) + J1(3,1,8) - J1(3,2,3) + J1(3,2,6) - J1(3,2,8)] - (\mathbf{p}_c \cdot \mathbf{q})^2 [J1(1,2,6) + J1(2,2,6) \\
& \left. + J1(3,2,3) - J1(3,2,6) + J1(3,2,8)] \right\}. \tag{A16}
\end{aligned}$$

- 
- [1] I. Adachi [Belle Collaboration], arXiv:1105.4583 [hep-ex].
- [2] A. Bondar *et al.* [Belle Collaboration], Phys. Rev. Lett. **108**, 122001 (2012).
- [3] D. Y. Chen and X. Liu, Phys. Rev. D **84**, 094003 (2011).
- [4] E. S. Swanson, Phys. Rev. D **91**, no. 3, 034009 (2015).
- [5] F. K. Guo, C. Hanhart, Q. Wang and Q. Zhao, Phys. Rev. D **91**, no. 5, 051504 (2015).
- [6] W. S. Huo and G. Y. Chen, Eur. Phys. J. C **76**, no. 3, 172 (2016).
- [7] F.-K. Guo, C. Hanhart, Y. S. Kalashnikova, P. Matuschek, R. V. Mizuk, A. V. Nefediev, Q. Wang and J.-L. Wynen, Phys. Rev. D **93**, no. 7, 074031 (2016).
- [8] Q. Wang, V. Baru, A. A. Filin, C. Hanhart, A. V. Nefediev and J.-L. Wynen, Phys. Rev. D **98**, no. 7, 074023 (2018).
- [9] Y. H. Chen, M. Cleven, J. T. Daub, F. K. Guo, C. Hanhart, B. Kubis, U. G. Meißner and B. S. Zou, Phys. Rev. D **95**, no. 3, 034022 (2017).

- [10] Y. H. Chen and F. K. Guo, arXiv:1906.05766 [hep-ph].
- [11] M. Cleven, F.-K. Guo, C. Hanhart, and U.-G. Meißner, Eur. Phys. J. A **47**, 120 (2011) [arXiv:1107.0254 [hep-ph]].
- [12] F.-K. Guo, C. Hanhart, and U.-G. Meißner, Phys. Rev. Lett. **103**, 082003 (2009); **104**, 109901(E) (2010) [arXiv:0907.0521 [hep-ph]].
- [13] S. Fleming and T. Mehen, Phys. Rev. D **78**, 094019 (2008) [arXiv:0807.2674 [hep-ph]].
- [14] G. Burdman and J. F. Donoghue, Phys. Lett. B **280**, 287 (1992).
- [15] M. B. Wise, Phys. Rev. D **45**, R2188 (1992).
- [16] T. M. Yan, H. Y. Cheng, C. Y. Cheung, G. L. Lin, Y. C. Lin, and H. L. Yu, Phys. Rev. D **46**, 1148 (1992); **55**, 5851(E) (1997).
- [17] R. Casalbuoni, A. Deandrea, N. Di Bartolomeo, R. Gatto, F. Feruglio, and G. Nardulli, Phys. Rept. **281**, 145 (1997) [arXiv:hep-ph/9605342].
- [18] F. Bernardoni *et al.* [ALPHA Collaboration], Phys. Lett. B **740**, 278 (2015) [arXiv:1404.6951 [hep-lat]].
- [19] F.-K. Guo, C. Hanhart, G. Li, U.-G. Meißner, and Q. Zhao, Phys. Rev. D **83**, 034013 (2011) [arXiv:1008.3632 [hep-ph]].
- [20] M. Cleven, Q. Wang, F.-K. Guo, C. Hanhart, U.-G. Meißner, and Q. Zhao, Phys. Rev. D **87**, 074006 (2013) [arXiv:1301.6461 [hep-ph]].
- [21] T. Mehen and J. W. Powell, Phys. Rev. D **88**, 034017 (2013) [arXiv:1306.5459 [hep-ph]].
- [22] I. Adachi *et al.* [Belle Collaboration], arXiv:1209.6450 [hep-ex].
- [23] Y.-H. Chen, J. T. Daub, F.-K. Guo, B. Kubis, U.-G. Meißner, and B.-S. Zou Phys. Rev. D **93**, 034030 (2016) [arXiv:1512.03583 [hep-ph]].
- [24] M. Tanabashi *et al.* [Particle Data Group Collaboration], Phys. Rev. D **98**, 030001 (2018).